Volume 8
Number 26
14 July 2020
Pages 5555–5784

Journal of Materials Chemistry B

Materials for biology and medicine

rsc.li/materials-b

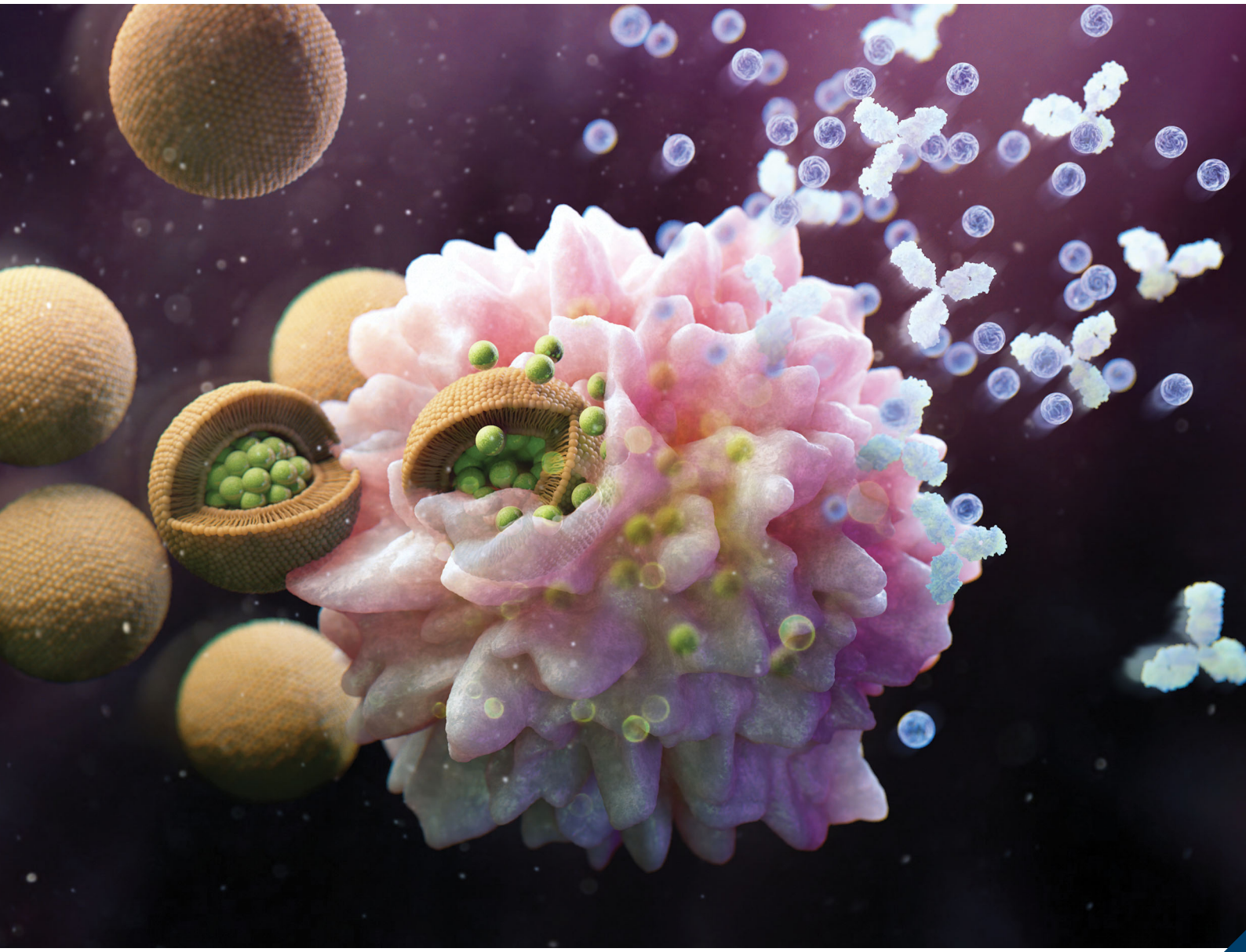

ISSN 2050-750X

ROYAL SOCIETY OF CHEMISTRY

PAPER

Daesub Song, Seungjoo Haam *et al.*
Co-delivery of antigens and immunostimulants *via* a polymersome for improvement of antigen-specific immune response

Indexed in Medline!

Journal of Materials Chemistry B

ROYAL SOCIETY OF CHEMISTRY

PAPER

Cite this: J. Mater. Chem. B, 2020, 8, 5620

Co-delivery of antigens and immunostimulants *via* a polymersome for improvement of antigen-specific immune response†

Jong-Woo Lim,‡[ab] Woonsung Na,‡[cd] Hyun-Ouk Kim,‡[e] Minjoo Yeom,[f] Aram Kang,[f] Geunseon Park,[a] Chaewon Park,[a] Jisun Ki,[a] Sojeong Lee,[a] Bud Jung,[f] Hyoung Hwa Jeong,[b] Daewon Park,[g] Daesub Song *[f] and Seungjoo Haam *[a]

Received 4th April 2020,
Accepted 29th May 2020

DOI: 10.1039/d0tb00892c

rsc.li/materials-b

Cellular uptake of antigens (Ags) by antigen-presenting cells (APCs) is vital for effective functioning of the immune system. Intramuscular or subcutaneous administration of vaccine Ags alone is not sufficient to elicit optimal immune responses. Thus, adjuvants are required to induce strong immunogenicity. Here, we developed nanoparticulate adjuvants that assemble into a bilayer spherical polymersome (PSome) to promote the cellular uptake of Ags by APCs. PSomes were synthesized by using a biodegradable and biocompatible block copolymer methoxy-poly(ethylene glycol)-*b*-poly(D,L-lactide) to encapsulate both hydrophilic and lipophilic biomacromolecules, such as ovalbumin (OVA) as a model Ag and monophosphoryl lipid A (MPLA) as an immunostimulant. After co-encapsulation of OVA and MPLA, the PSome synthetic vehicle exhibited the sustained release of OVA in cell environments and allowed efficient delivery of cargos into APCs. The administration of PSomes loaded with OVA and MPLA induced the production of interleukin-6 and tumor necrosis factor-alpha cytokines by macrophage activation *in vitro* and elicited effective Ag-specific antibody responses *in vivo*. These findings indicate that the nano-sized PSome may serve as a potent adjuvant for vaccine delivery systems to modulate enhanced immune responses.

Introduction

Vaccines are formulated from artificial or biosynthetic antigens mixed with adjuvants to induce protective immunity against external pathogens. Killed vaccines involve inactivation by heat or chemicals to ensure that the pathogen will not replicate in the host. For this reason, inactivated vaccines are safer than live attenuated vaccines.[1] However, the antigens (Ags) in inactivated vaccines elicit limited immunogenicity compared to other vaccine systems in generating robust T-cell mediated cellular responses as well as antibody-mediated humoral immunity. In addition, booster vaccinations are generally needed to induce long-lasting immunity.[2]

To increase the immunogenicity of vaccines, a variety of Ag vehicles are being developed.[3,4] Poor immunogenicity and non-existent cellular immune responses are due to the low efficiency of the uptake and processing of extracellular Ags by immune cells for presentation to naïve T cells. Recently, several nanoparticle based delivery systems are used for vaccines and immunotherapy.[5–10] Several different types of nanoparticles, such as micelles, liposomes, polymersomes, dendrimers, O/W emulsions, and virus-like particles, have been used as vaccine adjuvants to encapsulate either antigens or mixed with other molecules to enable antigen delivery and engineer specific immune responses.[11,12]

We developed an artificial nano-vesicle termed a polymersome (PSome). PSomes are self-assembled vesicles of a block amphiphilic copolymer, which offer some advantages as vaccine adjuvants.[13,14] They enhance the cellular uptake efficiency of Ags and induce the sustained release of Ags. PSomes contain aqueous cavities in their core, and their polymeric membrane acts as a physical barrier,[15,16] which allows the encapsulation, protection, and simultaneous delivery of hydrophilic and lipophilic molecules, such as Ags, adjuvants, proteins, peptides, and DNA and RNA fragments,

[a] Department of Chemical and Biomolecular Engineering, Yonsei University, Yonsei-ro 50, Seoul, 03722, Republic of Korea. E-mail: haam@yonsei.ac.kr
[b] Huvet Bio inc., 127 Beobwon-ro, Seoul, Republic of Korea
[c] College of Veterinary Medicine, Chonnam National University, Republic of Korea
[d] Animal Medical Institute, Chonnam National University, Gwangju, Republic of Korea
[e] Division of Chemical Engineering and Bioengineering College of Art, Kangwon National University, 1, Gangwondaehak-gil, Chuncheon-si, Gangwon-do, 24341, Republic of Korea
[f] College of Pharmacy, Korea University, Sejong-ro, Sejong 30019, Republic of Korea. E-mail: sds1@korea.ac.kr
[g] Department of Bioengineering, University of Colorado Denver Anschutz Medical Campus, USA

† Electronic supplementary information (ESI) available. See DOI: 10.1039/d0tb00892c
‡ These authors contributed equally.

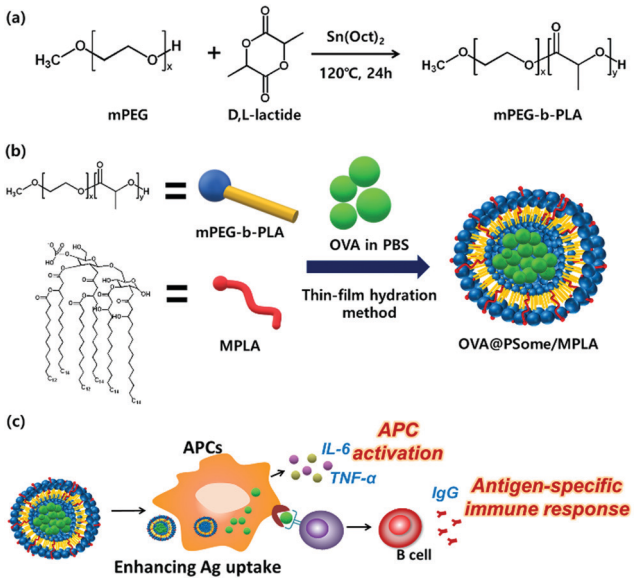

Scheme 1 Schematic diagram of the synthesis of (a) mPEG-*b*-PLA copolymers by ring-opening polymerization. (b) Design of a polymersome containing both OVA and MPLA (OVA@PSome/MPLA). (c) Illustration of enhanced cellular antigen (Ag) uptake by antigen-presenting cells (APCs) induced by OVA@PSome/MPLA, secretion of IL-6 and TNF-α by activated APCs, and Ag-specific antibody immune response-based humoral immunity.

without the additional need for chemical modification.[17–19] Despite the potential benefits of the encapsulation and sustained release of unmodified Ags or small adjuvants in these highly stable and tunable nano-vesicles, few studies have explored the development of the PSome as a vaccine delivery system.

We have previously described the formation of PSomes for the co-delivery of RNA and drugs using the biodegradable amphiphilic methoxy-poly(ethylene glycol)-*block*-poly(lactic acid) (mPEG-*b*-PLA) block copolymer.[20] Here, we prepared mPEG-*b*-PLA based PSomes co-encapsulated with ovalbumin (OVA) as a model Ag, as well as the monophosphoryl lipid A (MPLA) immunostimulant (OVA@PSomes/MPLA). The ability of OVA@PSomes/MPLA to potentiate robust immune responses after their cellular internalization was investigated *in vitro* and *in vivo* (Scheme 1).

PSomes were synthesized by adjusting the ratio of the hydrophobic to the hydrophilic constituents of the block copolymer to form vesicles bounded by a bilayer membrane. The vesicles had an average diameter of approximately 100 nm in aqueous solution. The PSomes displayed the sustained release of OVA conjugated with fluorescein isothiocyanate (FITC) in cell environments, which prolonged the retention time of Ags during cellular uptake by antigen-presenting cells (APCs) and significantly enhanced the stability and delivery efficacy of the Ag and MPLA into APCs.[21–23] Finally, *in vitro* and *in vivo* studies of the PSome were carried out to assess the efficacy of APC maturation in macrophages and the production of Ag-specific antibodies in mice after intramuscular vaccination. PSomes induced Ag-specific humoral immune responses *in vivo*. The collective results indicate the potential of PSomes as a potent vaccine adjuvant system.

Results and discussion

Characteristics of the copolymer and PSome

To utilize PSome-based nanoparticulate adjuvants for Ag delivery with the MPLA immunostimulatory lipid, we prepared an amphiphilic copolymer mPEG-*b*-PLA, whose biodegradability and biocompatibility are suitable for medical applications. The biocompatible copolymer mPEG-*b*-PLA was obtained by ring-opening polymerization of D,L-lactide monomers with hydroxyl groups at the ends of mPEG in toluene for 24 h, followed by repeated precipitation. The successful polymerization of mPEG-*b*-PLA was confirmed by ^{1}H-NMR and FT-IR.[26]

Fig. 1(a) shows the FT-IR spectra of mPEG and mPEG–PLA. The strong absorption at 1760 cm^{-1} is assigned to the –C═O stretch of PLA, while the bands at 2902 and 1470 cm^{-1} are due to –O–CH$_3$ and –OH stretch of PEG and PLA, respectively. The block length of mPEG-*b*-PLA could be adjusted by changing the molar ratio of D,L-lactide to mPEG (mPEG-*b*-PLA#1 and #2). The average molecular weight of the mPEG-*b*-PLA was calculated by comparing the integrated-area of the peak at 5.17 ppm (CH in PLA) with that of the peak at 3.38 ppm (CH$_3$O in mPEG) in NMR analysis (Table S1, Fig. 1(b)). The molecular weight of mPEG-*b*-PLA was determined by gel permeation chromatography (GPC), with calibration by polystyrene standards (Table S1, ESI†). As shown in Fig. 1(c), single peaks were evident in the GPC of mPEG-*b*-PLA. These results demonstrated that the D,L-lactide successfully polymerized to mPEG, and the homopolymerization of D,L-lactide did not occur during the reaction.

PSomes were synthesized using the thin film hydration method by loading OVA and MPLA into mPEG-*b*-PLA. Two types of PSomes (OVA@PSomes#1/MPLA and OVA@PSomes#2/MPLA) were prepared to prepare bilayer vesicles. Introduction of external forces that included magnetic stirring and ultrasonication induced the formation of spherical submicron-sized

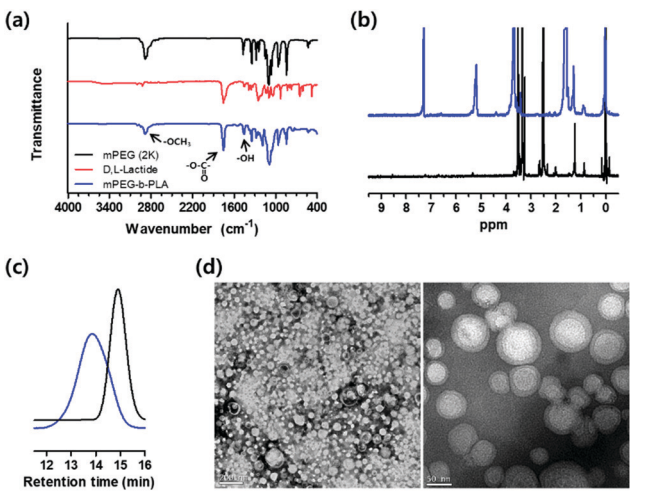

Fig. 1 (a) FT-IR, (b) ^{1}H-NMR, and (c) gel permeation chromatography (GPC) spectra of mPEG (black), D,L-lactide (red), and mPEG-*b*-PLA (blue). (d) Representative TEM images of OVA@PSome#1/MPLA (left) and OVA@PSome#2/MPLA (right). Scale bars denote 200 nm and 50 nm, respectively.

PSomes and enhanced the homogeneity (OVA@PSomes#1/MPLA: 70.4 ± 32.3 nm and OVA@PSomes#2MPLA: 98.9 ± 31.7 nm) (Table S2, ESI†). PSomes stored at 4 °C remained stable for over 14 days. The zeta potentials of the PSomes were negative owing to the hydroxyl groups of PLA (OVA@PSomes#1/MPLA: −12.38 mV and OVA@PSomes#2/MPLA: −14.73 mV). TEM of PSomes revealed the bilayer structure of PSomes#2 and micellar nanoparticles of PSomes#1 (Fig. 1(d)). PSomes#2 had a bilayer core/shell structure for the loading of OVA and MPLA, as well as the narrowest homogeneity with a polydispersity index of 0.093. Thus, we used PSomes#2 for the antigen cellular delivery platform and as a nanoparticulate adjuvant.

Release profiles of OVA-FITC

We investigated whether PSomes enabled increased Ag retention in the cellular microenvironments. OVA-FITC was encapsulated in PSomes, and the kinetics of OVA-FITC release at 37 °C in the medium was quantified on the basis of fluorescence intensity. As shown in Fig. 2, OVA-FITC-only groups quickly released their entire payload of loaded OVA-FITC within approximately 1 h. However, PSomes showed a sustained release profile and a noticeably enhanced retention of OVA-FITC, releasing only half of their entire payload by approximately 3 h. The findings indicated that PSomes can increase the duration of Ag release. This prolonged Ag presentation might potently induce Ag-specific immune responses.[27,28]

Cellular toxicity and OVA uptake efficacy of PSomes *in vitro*

To verify the potential cytotoxicity of PSomes and mPEG-*b*-PLA, we carried out an *in vitro* cell viability assay using a cell counting kit. Fig. S1 (ESI†) shows the viability of RAW264.7 macrophages treated with PSomes and mPEG-*b*-PLA (0.001 to 1 mg ml^{-1}). PSomes and mPEG-*b*-PLA showed no significant toxicity up to 1 mg ml^{-1}. mPEG-*b*-PLA is well known for its biodegradability and biocompatibility.[29,30]

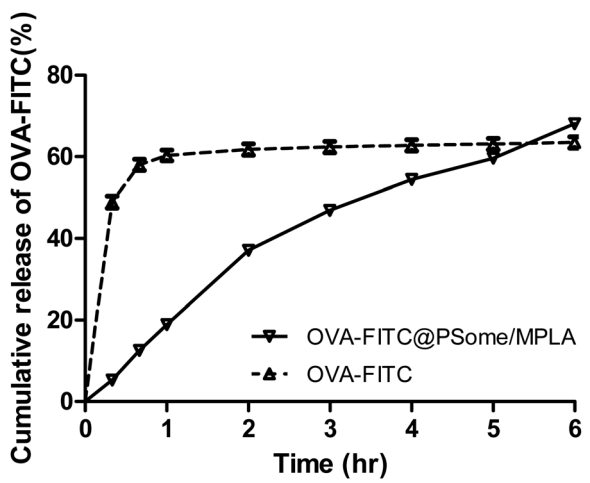

Fig. 2 Release profiles of OVA-FITC from OVA-FITC@PSome/MPLA and OVA-FIC-only in PBS (pH 7.4) at 37 °C. Data are presented as mean ± S.D. (n = 3).

Ag cellular uptake by APCs is an important step to elicit strong immune responses. Therefore, we investigated the intracellular Ag uptake efficiency of PSomes as a vaccine delivery system *in vitro*. The macrophage is a major cell of the immune system, which functions to present foreign Ags to helper T cells and particulate Ag in the form of immune complexes to B cells. To conduct the assay under standard conditions, we used RAW264.7 macrophages, since they are one of the most commonly used myeloid cell types.[31] OVA was used a model Ag and FITC as a tracker. PSomes loaded with OVA-FITC (OVA-FITC@PSome/MPLA) were incubated with RAW264.7 cells for 6 h and examined by CLSM. As shown in Fig. 3(a), a strong fluorescence image of OVA-FITC was visualized in the cytoplasm of OVA-FITC@PSomes/MPLA, indicating that the PSomes were readily internalized into the cells and released their payload of OVA-FITC. Separate fluorescence due to OVA-FITC (green) and lysosomes (red) was observed using Lysotracker to visualize the lysosomes of macrophages.[32,33] These results suggested that OVA-FITC was released in the cytoplasm of the cells and that successful delivery of OVA-FITC@PSome/MPLA occurred. This finding was consistent with an earlier report that PSomes synthesized by using mPEG-*b*-PLA can degrade in the endosomal environment.[20] In contrast, weaker fluorescence was produced by the OVA-FITC-only control, because of its low cellular uptake efficiency. As a quantitative analysis, the fluorescence expression level of OVA-FITC in RAW264.7 cells was measured by flow cytometry. As shown in Fig. 3(b), a significant increase in OVA-FITC fluorescence intensity was observed for the groups treated with PSomes compared to those treated with OVA-FITC-only. The use of OVA-FITC@PSome/MPLA led to enhanced localization of OVA-FITC (approximately 2.9-fold) in macrophages compared with OVA-FIC after a 6 h incubation. Overall, the results demonstrated the potential of PSomes as a carrier for intracellular Ag delivery.

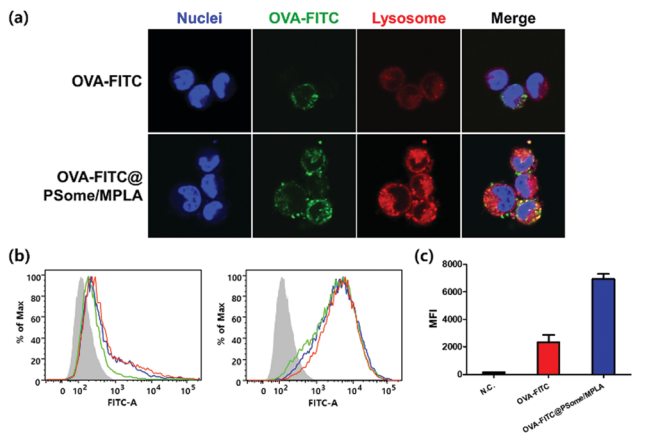

Fig. 3 (a) Fluorescence images of RAW264.7 cells treated with a mixture of OVA-FITC-only and OVA-FITC@PSome/MPLA for 6 h at 37 °C. Scale bar = 5 μm. Antigen cellular uptake efficiency was measured by OVA-FITC-positive cells using flow cytometry. (b) OVA-FITC-only (left) and OVA-FITC@PSome/MPLA (right) were used to treat RAW264.7 macrophages for 6 h at 37 °C. Gray, blue, green, and red histograms represent the cells treated with negative control and each sample, respectively. (c) Median fluorescence intensity (MFI) for each treatment group (mean ± S.D., n = 3).

Secretion of immunostimulatory cytokines by APC activation

Next, we explored the potential of OVA-FITC@PSome/MPLA with mature APCs *in vitro*. We prepared vesicles co-delivering the OVA model Ag and the MPLA biomolecular adjuvant. MPLA is a Food and Drug Administration approved toll-like receptor 4 agonist adjuvant, which amplifies vaccine immunogenicity.[34] PSomes containing both OVA and MPLA (OVA@PSome/MPLA) were treated with RAW264.7 macrophages for 6 h, and the secretions of the IL-6 and TNF-α immunostimulatory cytokines were analyzed by ELISA. OVA@PSome/MPLA produced significantly higher induction of IL-6 and TNF-α (5.75-fold and 9.9-fold, respectively) than OVA-only, and 3.31-fold and 5.34-fold, respectively, compared with OVA/MPLA (Fig. 4). To determine the influence of PSome vesicles on the inflammatory responses, we incubated PSomes with macrophages using a concentration of PSomes that was equivalent to the concentration of OVA@PSome/MPLA. The PSome samples showed low secretion of IL-6 and TNF-α, compared with OVA@PSome/MPLA and OVA/MPLA. These results indicated that the immunostimulatory cytokines secreted from OVA@PSome/MPLA were not induced by the inflammatory response of PSomes, but rather were due to efficient cellular uptake of both OVA and MPLA by PSomes. Additionally, we analyze the *in vitro* test using another mouse alveolar macrophage cell (MH-S). As shown in Fig. S3 (ESI†), OVA@PSome/MPLA produced significantly higher induction of IL-6 than OVA only and OVA/MPLA (1.25-fold and 1.34-fold, respectively). There was no significant difference between OVA only and OVA/MPLA, but when loaded and processed in PSomes, immune-stimulatory cytokine secretion by macrophage activation was much amplified. Delivery of Ags and immunostimulatory adjuvants to APCs using nanoparticles has also been reported as an effective strategy to upregulate vaccine immunogenicity.[35,36] These results demonstrated that PSomes enhanced cell uptake efficiency, which might also lead to increased immunostimulatory activity by mature APCs.

OVA-specific immune response elicited by PSomes *in vivo*

Considering the *in vitro* findings that improved co-delivery of Ags and adjuvants induced IL-6 and TNF-α secretion, we examined the *in vivo* immune-stimulatory effect after vaccination with

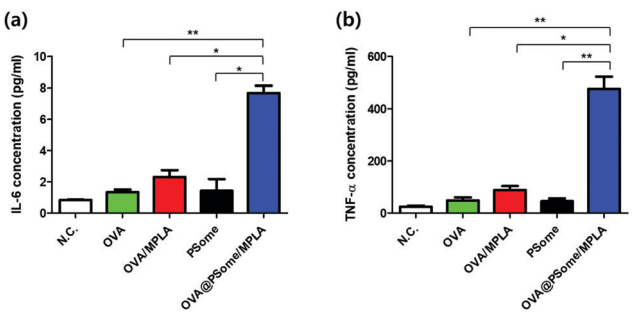

Fig. 4 Quantitative comparison of (a) IL-6 and (b) TNF-α induction in RAW264.7 cells. Expression levels of IL-6 and TNF-α in macrophages stimulated with OVA-only (2.5 μg), OVA (2.5 μg)/MPLA (0.4 μg), PSome (83 μg), and OVA (2.5 μg)@PSome (83 μg)/MPLA (0.4 μg). The expression level of IL-6 and TNF-α in the supernatants was determined by ELISA. Student's *t*-test and one-way ANOVA were used for statistical analysis. Data are presented as mean ± S.E.M. (n = 3; $*p < 0.01$, $**p < 0.001$).

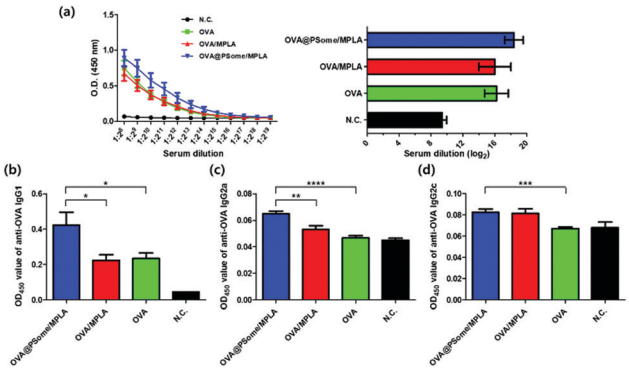

Fig. 5 Quantitative comparison of OVA-specific antibody induction in mice (n = 5 for each group) 2 weeks after the final vaccination. Induction of OVA-specific (a) serum total IgG, and (b) IgG1, (c) IgG2a, and (d) IgG2c in mice vaccinated with OVA-only (20 mg), OVA/MPLA, and OVA@PSome/MPLA were determined using ELISA. Student's *t*-test and one-way ANOVA were used for statistical analysis. Data are presented as mean ± S.E.M. ($*p < 0.05$, $**p < 0.01$, $***p < 0.001$, $****p < 0.0001$).

PSomes. To investigate the induction of OVA-specific antibody responses, the sera of immunized mice were collected 2 weeks after the first and final vaccinations, and the antibody level was analyzed by ELISA. As shown in Fig. S2 (ESI†), there was no significant difference among groups 2 weeks after the first vaccination. However, after booster doses, OVA@PSome/MPLA immunized mice generated significantly higher titers of OVA-specific total IgG responses than all controls (Fig. 5(a) and (b)). The booster administration was an effective immunization method to generate better antibody responses (Fig. S2, ESI†). Mouse vaccination with OVA@PSomes/MPLA produced higher levels of IgG2a and IgG2c, which are Th1-type antibodies, as well as the IgG1, a Th2-type antibody, than mouse vaccination with OVA/MPLA and OVA-only (Fig. 5(c) and (d)). Further, we tested the adjuvant function of PSomes with influenza virus antigen (A/canine/VC378/2012, cH3N2). Two weeks after the final vaccination, the sera from each group of mice were obtained and the levels of cH3N2-specific Ab were determined by ELISA. Fig. S4 (ESI†) shows that vaccination with Ag@PSome/MPLA induced the highest levels of Ag-specific IgG in the sera of mice. The enhanced immune responses may have occurred because the Ag was protected from degradation, its release was sustained, and its cellular delivery was improved using PSomes. Notably, the OVA-specific IgG level was higher when vaccinated with the Ag and adjuvant co-encapsulated PSome (OVA@PSome/MPLA) than soluble OVA together with free MPLA (OVA/MPLA). These data implied that the Ag delivery system encapsulating a toll-like receptor agonist could serve as a promising strategy to induce potent cellular immunity as well as humoral immunity.

Experimental

Materials

Methoxy-poly(ethylene glycol) (mPEG) with a molecular weight of 2000 Da, D,L-lactide (3,6-dimethyl-1,4-dioxane-2,5-dione), and stannous octoate ($Sn(Oct)_2$) were obtained from Sigma-Aldrich

(St. Louis, MO, USA). Phosphate buffered saline (PBS; 10 mM, pH 7.4) was purchased from Welgene (Gyeongsan, South Korea). Dulbecco's modified Eagle's medium (DMEM), OVA, and OVA-FITC were obtained from Thermo Fisher Scientific (Waltham, MA, USA). MPLA was obtained from Invivogen (San Diego, CA, USA). Horseradish peroxidase (HRP)-conjugated goat anti-mouse IgG, IgG1, IgG2a, and IgG2c antibodies were purchased from Abcam (Cambridge, UK). All other chemicals and reagents were of analytical grade.

Synthesis of amphiphilic copolymer and preparation of OVA@PSome

The mPEG-*b*-PLA copolymers were synthesized by ring-opening polymerization of D,L-lactide as previously described.[20,24] A series of mPEG-*b*-PLA copolymers with varying mass fractions of mPEG (0.278 and 0.385) were synthesized by ring-opening polymerization of D,L-lactide with hydroxyl-terminated mPEG as an initiator and $Sn(Oct)_2$ as a catalyst. mPEG was introduced into a three-neck flask along with anhydrous toluene. Various concentrations of D,L-lactide and $Sn(Oct)_2$ (0.05 wt% of mPEG and D,L-lactide) were then injected into the flask, and the reaction mixture was heated with reflux at 120 °C overnight under a nitrogen atmosphere. After the reaction was completed, the product solution was removed by rotary evaporation and precipitated in excess cold diethyl ether to produce mPEG-*b*-PLA. The copolymer products were filtered using a Buchner funnel and vacuum-dried at room temperature for 1 day. The molecular weight and the mPEG content of the synthesized mPEG-*b*-PLA were determined by ^{1}H nuclear magnetic resonance (NMR) spectra using a 400 MHz NMR spectrometer (Bruker, Bremen, Germany) and gel permeation chromatography (YOUNG LIN ACME HPLC System, Young Lin Instrument Co., Korea). Their chemical structures were analyzed using Fourier transform-infrared (FT-IR) spectra (Excalibur Series, Varian Inc., Palo Alto, CA, USA).

To prepare the OVA and MPLA co-encapsulated PSomes (OVA@PSome/MPLA), 10 mg of mPEG-*b*-PLA copolymer and MPLA was dissolved in 1 ml of chloroform. The chloroform was removed using a rotary evaporator to form a thin film of the mPEG-*b*-PLA copolymer and MPLA on the wall of the flask, which was placed under high vacuum for over 6 h to remove any residual solution. The dried film was hydrated in a solution of OVA dissolved in 2 ml of PBS for 6 h at 50 °C and magnetically stirred for an additional 12 h.[17,19,20] After stirring, the solution was ultra-sonicated using a model SH-2199 instrument (Sae Han, Seoul, Korea) at 190 W for 30 min. Finally, the solution was transferred for dialysis in PBS with a molecular weight cut-off of 100 kDa for 24 h. OVA@PSome and PSome were synthesized as described for OVA@PSome/MPLA, except for encapsulation of MPLA or both OVA and MPLA, respectively. The size distribution and zeta potential of the OVA@PSome/MPLA and PSome/MPLA were measured using dynamic laser scattering and zeta potential analysis (ELS-Z; Otsuka Electronics, Osaka, Japan), respectively, and their morphology was investigated by transmission electron microscopy (TEM) using a JEM-1011 microscope (JEOL, Tokyo, Japan).

Controlled release test of OVA-FITC

To investigate the release profiles of OVA from PSomes, we first prepared OVA-FITC@PSome/MPLA as detailed above by substituting OVA as OVA-FITC. OVA-FITC@PSome/MPLA and OVA-FITC solutions were sealed in two different dialysis tubes with a molecular weight cut-off of 100 kDa and then immersed in 5 ml PBS at 37 °C with moderate shaking.[25] At regular time intervals, volumes of the solutions from each dialysis tube were collected separately for quantification of fluorescence. An equal volume of fresh medium was added as a replacement for continued profiling of OVA-FITC release. The amount of released OVA-FITC was monitored for 6 h by measuring the fluorescence intensity of OVA-FITC at 480 nm excitation and 525 nm emission wavelengths. An OVA-FITC-only group was used for control experiments.

In vitro cytotoxicity test and analysis of OVA cell uptake

RAW264.7 macrophage cells (4×10^5) were seeded onto covered glass-bottom dishes (SPL Life Sciences Co, Ltd, Pocheon, South Korea) and then incubated at 37 °C in an atmosphere of 5% CO_2. After 24 h, the cells were treated with OVA-FITC@PSome/MPLA and OVA-FITC solution and incubated at 37 °C in 5% CO_2 for 6 h. After the PSome incubation, the cells were washed with PBS, and the cell uptake of the particles was visualized using confocal laser scanning microscopy (LSM700; Carl Zeiss, Jena, Germany). The cells were stained with Hoechst (Molecular Probes, Eugene, OR, USA) to visualize the nucleus and LysoTracker Red DND-99 (Molecular Probes) to visualize the lysosomes.

For flow cytometry analysis, RAW264.7 cells (4×10^5) were seeded in 6-well plates and incubated for 24 h at 37 °C in an atmosphere of 5% CO_2. After 24 h, OVA-FITC@PSome/MPLA and OVA-FITC solutions were added, and the cells were incubated at 37 °C with 5% CO_2 for 6 h. The harvested cells after treatment were washed and collected with blocking buffer (PBS, pH 7.4, containing 1% bovine serum albumin (BSA) and 0.1% sodium azide). Flow cytometry was performed on an LSR II flow cytometer (BD Biosciences, Santa Clara, CA, USA) and analyzed using FlowJo software.

In vitro analysis of interleukin-6 (IL-6) and tumor necrosis factor-alpha (TNF-α) secretion levels by enzyme-linked immunosorbent assay (ELISA)

RAW264.7 or MH-S mouse macrophages were prepared according to conventional protocols and cultured in DMEM or RPMI1640 containing 10% fetal bovine serum. Cells in 96-well plates (2×10^4 cells per well) were stimulated with PBS or different concentrations of OVA alone, OVA/MPLA, PSome alone, or OVA@PSome/MPLA for 6 h. Supernatants were collected, and IL-6 and TNF-α were quantified using an ELISA kit (Invitrogen, Carlsbad, CA, USA).

Animals and vaccine

Six-week-old female C57BL/6 mice were intramuscularly injected in the caudal thigh. Two-dose immunization was administered two weeks apart with or without adjuvants: PBS, OVA alone,

OVA/MPLA, or OVA@PSome/MPLA. The influenza viruses A/canine/Korea/01/2007 (cH3N2) were propagated in MDCK cells, which were grown in DMEM containing 1 μg ml^{-1} TPCK-trypsin (Thermo Fisher Scientific, Waltham, MA, USA) and supplemented with 1% antibiotic–antimycotic at 37 °C and 5% CO_2. Inactivated cH3N2 was incubated for 18 h at 37 °C with a 0.2% final concentration of formalin. Mice were vaccinated *via* intramuscular injection twice at 2 week intervals with inactivated cH3N2 (Ag) alone, Ag/MPLA or, Ag@PSome/MPLA. Blood was collected from the mice *via* the retro-orbital plexus two weeks after the final injection. All experimental procedures were approved by the Chonnam National University Institutional Animal Care and Use Committee (approval number: CNU IACUC-YB-2019-84, date of approval: November 7, 2019).

Ag-specific antibody response using ELISA

The sera were obtained from the blood by centrifugation for 20 min at 13 000 rpm. Antigen-specific IgG, IgG1, IgG2a, and IgG2c antibody titers were determined by ELISA using serum samples from each mouse (n = 5). In particular, 96-well immunoplates (SPL Life Sciences, Gyeonggi, Korea) were incubated with 100 μl of OVA or cH3N2 overnight at 4 °C. After blocking for 1 h at 37 °C in 5% skim milk in PBS-Tween, 100 μl of each serum sample serially two-fold diluted with 3% skim milk was treated in OVA or Ag coated immunoplates and incubated (1 h at 37 °C). Next, HRP-conjugated goat anti-mouse IgG, IgG1, IgG2a, or IgG2c antibodies (Abcam) diluted 1 : 50 000 in 3% skim milk were added in immunoplates. Each step featured three to five washes with 0.05% Tween 20 in PBS. After incubation at room temperature for 1 h, 100 μl of TMB Substrate Reagent (BD Biosciences) was added to each well. The reaction was stopped by adding 2 N sulfuric acid. The absorbance was recorded by using a SpectraMAX i3x Multi-Mode Detection Platform microplate reader (Molecular Devices, Sunnyvale, CA, USA) at a wavelength of 450 nm. The endpoint titer was determined using an optical density cut-off value.

Conclusions

PSome-based nanoparticulate adjuvants were designed for the co-delivery of an Ag and an immunostimulant. The PSomes were confirmed to be potent vaccine adjuvants capable of generating strong immune responses. To optimize the synthesis of spherical bilayer nanoparticles, we adjusted the block length of the amphiphilic copolymer (mPEG-*b*-PLA) and prepared nano-sized PSomes for the delivery of both hydrophilic Ags and lipophilic immunostimulants. PSomes induced better Ag cellular uptake by APCs than soluble Ag groups and allowed sustained release of Ags in cellular microenvironments. The improved retention time, sustained release of Ags, and enhanced cellular Ag uptake using PSomes led to the activation of APCs that secreted immunostimulatory cytokines (IL-6 and TNF-α). The engineered Ag delivery system also induced robust Ag-specific antibody responses *in vivo*. Collectively, these findings suggest that PSomes that co-encapsulate an Ag and a toll-like receptor agonist may be potent vaccine delivery vehicles capable of achieving robust immune responses. The present findings will help design novel vaccination strategies against infectious diseases.

Author contributions

J.-W. Lim, W. Na and H.-O. Kim developed the basic concept, performed the experiments, analyzed the data, and wrote the paper. M. Yeom, A. Kang, G. Park, C. Park, J. Ki, S. Lee and B. Jung directed and performed the analysis of experiments and quality control samples. H. H. Jeong and D. Park revised the paper. S. Haam and D. Song contributed to supervision, had the idea for the project, and directed the project. All authors reviewed the paper.

Conflicts of interest

There are no conflicts to declare.

Acknowledgements

This research was supported by the Bio & Medical Technology Development Program of the National Research Foundation (NRF) funded by the Ministry of Science & ICT (NRF-2018 M3A9H4056340). This research was supported by the Nano·Material Technology Development Program through the National Research Foundation of Korea (NRF) funded by the Ministry of Education, Science and Technology (Grant number: 2017M3A7B4041798). This research was supported by a grant of the Korea Health Technology R&D Project through the Korea Health Industry Development Institute (KHIDI), funded by the Ministry of Health & Welfare, Republic of Korea (grant number: HI18C1159).

Notes and references

1 S. M. Kaech, E. J. Wherry and R. Ahmed, *Nat. Rev. Immunol.*, 2002, **2**, 251–262.
2 M. M. Levine and M. B. Sztein, *Nat. Immunol.*, 2004, **5**, 460–464.
3 B. C. Buckland, *Nat. Med.*, 2005, **11**, S16–19.
4 J. W. Lim, W. Na, H. O. Kim, M. Yeom, G. Park, A. Kang, H. Chun, C. Park, S. Oh, V. P. Le, H. H. Jeong, D. Song and S. Haam, *Adv. Healthcare Mater.*, 2019, **8**, e1800953.
5 H. Wang and D. J. Mooney, *Nat. Mater.*, 2018, **17**, 761–772.
6 H. Phuengkham, L. Ren, I. W. Shin and Y. T. Lim, *Adv. Mater.*, 2019, **31**, e1803322.
7 P. Yang, H. Song, Y. Qin, P. Huang, C. Zhang, D. Kong and W. Wang, *Nano Lett.*, 2018, **18**, 4377–4385.
8 A. S. Cheung and D. J. Mooney, *Nano Today*, 2015, **10**, 511–531.
9 P. Huang, X. Wang, X. Liang, J. Yang, C. Zhang, D. Kong and W. Wang, *Acta Biomater.*, 2019, **85**, 1–26.
10 S. Talebian, J. Foroughi, S. J. Wade, K. L. Vine, A. Dolatshahi-Pirouz, M. Mehrali, J. Conde and G. G. Wallace, *Adv. Mater.*, 2018, **30**, e1706665.

11 D. M. Smith, J. K. Simon and J. R. Baker, Jr., *Nat. Rev. Immunol.*, 2013, **13**, 592–605.
12 L. Zhao, A. Seth, N. Wibowo, C. X. Zhao, N. Mitter, C. Yu and A. P. Middelberg, *Vaccine*, 2014, **32**, 327–337.
13 D. A. Christian, S. Cai, D. M. Bowen, Y. Kim, J. D. Pajerowski and D. E. Discher, *Eur. J. Pharm. Biopharm.*, 2009, **71**, 463–474.
14 K. T. Kim, J. J. L. M. Cornelissen, R. J. M. Nolte and J. C. M. van Hest, *Adv. Mater.*, 2009, **21**, 2787–2791.
15 R. Chandrawati and F. Caruso, *Langmuir*, 2012, **28**, 13798–13807.
16 M. S. Kim and D. S. Lee, *Chem. Commun.*, 2010, **46**, 4481–4483.
17 H.-O. Kim, J.-W. Lim, J. Choi, H. Lee, H. Y. Son, J. Kim, G. Park, H. Chun, D. Song, Y.-M. Huh and S. Haam, *J. Mater. Chem. B*, 2017, **5**, 9571–9578.
18 H.-O. Kim, W. Na, M. Yeom, J. Choi, J. Kim, J.-W. Lim, D. Yun, H. Chun, G. Park, C. Park, J.-K. Kim, D. G. Jeong, V. P. Le, K. Lee, J. M. Lee, H. H. Jeong, D. Song and S. Haam, *Adv. Funct. Mater.*, 2018, **28**, 1800960.
19 H. Chun, M. Yeom, H.-O. Kim, J.-W. Lim, W. Na, G. Park, C. Park, A. Kang, D. Yun, J. Kim, D. Song and S. Haam, *Polym. Chem.*, 2018, **9**, 2116–2123.
20 H. O. Kim, E. Kim, Y. An, J. Choi, E. Jang, E. B. Choi, A. Kukreja, M. H. Kim, B. Kang, D. J. Kim, J. S. Suh, Y. M. Huh and S. Haam, *Macromol. Biosci.*, 2013, **13**, 745–754.
21 W. Li, S. Liu, H. Yao, G. Liao, Z. Si, X. Gong, L. Ren and L. Wang, *J. Colloid Interface Sci.*, 2017, **508**, 145–153.
22 M. Hamidi, M. A. Shahbazi and K. Rostamizadeh, *Macromol. Biosci.*, 2012, **12**, 144–164.
23 C. Martin, N. Aibani, J. F. Callan and B. Callan, *Ther. Delivery*, 2016, **7**, 15–31.
24 S. Kaihara, S. Matsumura, A. G. Mikos and J. P. Fisher, *Nat. Protoc.*, 2007, **2**, 2767–2771.
25 J. J. Moon, H. Suh, A. Bershteyn, M. T. Stephan, H. Liu, B. Huang, M. Sohail, S. Luo, S. H. Um, H. Khant, J. T. Goodwin, J. Ramos, W. Chiu and D. J. Irvine, *Nat. Mater.*, 2011, **10**, 243–251.
26 K.-Y. Lee, Y.-T. Chiu and C.-L. Lo, *RSC Adv.*, 2015, **5**, 83825–83836.
27 Y. Men, B. Gander, H. P. Merkle and G. Corradin, *Vaccine*, 1996, **14**, 1442–1450.
28 H. H. Tam, M. B. Melo, M. Kang, J. M. Pelet, V. M. Ruda, M. H. Foley, J. K. Hu, S. Kumari, J. Crampton, A. D. Baldeon, R. W. Sanders, J. P. Moore, S. Crotty, R. Langer, D. G. Anderson, A. K. Chakraborty and D. J. Irvine, *Proc. Natl. Acad. Sci. U. S. A.*, 2016, **113**, E6639–E6648.
29 B. Tyler, D. Gullotti, A. Mangraviti, T. Utsuki and H. Brem, *Adv. Drug Delivery Rev.*, 2016, **107**, 163–175.
30 J. K. Oh, *Soft Matter*, 2011, **7**, 5096–5108.
31 L. Martinez-Pomares and S. Gordon, *Cell*, 2007, **131**, 641–643.
32 E. Jang, E. Kim, H. Y. Son, E. K. Lim, H. Lee, Y. Choi, K. Park, S. Han, J. S. Suh, Y. M. Huh and S. Haam, *Biomaterials*, 2016, **105**, 12–24.
33 E. B. Choi, J. Choi, S. R. Bae, H.-O. Kim, E. Jang, B. Kang, M.-H. Kim, B. Kim, J.-S. Suh, K. Lee, Y.-M. Huh and S. Haam, *Nano Res.*, 2014, **8**, 1169–1179.
34 V. Mata-Haro, C. Cekic, M. Martin, P. M. Chilton, C. R. Casella and T. C. Mitchell, *Science*, 2007, **316**, 1628–1632.
35 Y. Tao, E. Ju, Z. Li, J. Ren and X. Qu, *Adv. Funct. Mater.*, 2014, **24**, 1004–1010.
36 H. Jiang, Q. Wang, L. Li, Q. Zeng, H. Li, T. Gong, Z. Zhang and X. Sun, *Adv. Sci.*, 2018, **5**, 1700426.